International Journal of Engineering Sciences & Research Technology

(A Peer Reviewed Online Journal)
Impact Factor: 5.164

IJESRT

RESEARCHERID
THOMSON REUTERS

[Tubreoumya *et al.*, 11(2): February, 2022]
IC™ Value: 3.00

ISSN: 2277-9655
Impact Factor: 5.164
CODEN: IJESS7

IJESRT
INTERNATIONAL JOURNAL OF ENGINEERING SCIENCES & RESEARCH TECHNOLOGY

ENERGY ANALYSIS OF THE PERFORMANCE OF A SOLAR ADSORPTION REFRIGERATOR

Guy Christian Tubreoumya*[1,2], Sidpouita Mathilde Koudougou[1], Jacques Nebié[1,2], Téré Dabilgou[1,2] Eloi Salmwendé Tiendrebeogo[1], Belkacem Zeghmati[2], Alfa Oumar Dissa[1], Jean Koulidiati[1] & Antoine Bere[1]

[1]Laboratoire de Physique et de Chimie de l'Environnement (LPCE), Université Joseph Ki Zerbo, Ouagadougou, Burkina Faso.

[2]LAboratoire de Mathématiques et Physique (LA.M.P.S), Université de Perpignan Via Domitia (UPVD).

DOI: 10.29121/ijesrt.v11.i2.2022.3

ABSTRACT

This paper presents a contribution to the study of the process of cold production by adsorption from solar energy. This study mainly includes a modeling, simulation and sizing study of an adsorption solar refrigerator using the zeolite-water couple. For this purpose, a mathematical model of heat and mass transfers in each component of the adsorption solar refrigerator was developed. The results show that the performance of the adsorption solar refrigerator depends on several parameters. For example, with a maximum solar radiation of 990W/m^2, the maximum temperatures of the absorber plate, zeolite and condenser are 396 K (123°C), 395 K (122°C) and 320 K (47°C), respectively. The evaporator temperature can drop to a minimum temperature of 276 K (3°C). Furthermore, the simulation showed that the climatic conditions also have a great influence on the operation of the solar refrigerator. Thus, the amounts of cold produced, the average solar flux densities and the COPs during March and December are 6.391 MJ and 4.642 MJ, 590 W/m^2 and 514 W/m^2 and 0.25 and 0.21, respectively, relative to the values of the climate parameters. Similarly, with a daily average solar flux density of 436 W/m^2 and 480 W/m^2 respectively for the months of August and October, the COPs are 0.11 and 0.15 respectively, with a total amount of cold produced of 2.12 and 3.1 MJ respectively.

KEYWORDS: Solar refrigeration, Adsorption, Simulation, Zeolite/Water, Heat and mass transfer.

1. INTRODUCTION

Compressor cooling systems are the most widely used cooling systems because of the numerous cooling requirements. Indeed, the use of cold is sought for the conservation of food and pharmaceutical products, the conservation of crop products (tomatoes, onions, potatoes etc.) and also the air conditioning of buildings. These systems consume excessive electrical energy and use refrigerants such as CFCs (chlorofluorocarbons), HCFCs (hydrochlorofluorocarbons) and HFCs (hydrofluorocarbons) etc. These fluids are harmful to the ozone layer and contribute to the greenhouse effect. This is why the international agreements of the Montreal protocol in 1987 recommend the reduction of the use of these refrigerants [1]. Solar adsorption refrigeration systems are cold production systems that use solar energy as an energy source. They also use refrigerants such as water, ammonia and methanol which have a low effect on the environment [2-4]. Thus, this type of system constitutes a valid alternative to compression systems, which is both ecological and energetic. The energy deficit in Burkina Faso is very high and several areas do not have access to the electrical network. However, the country has a good sunshine with an average irradiation between 5.5 kWh.m^{-2}day^{-1} and 6.5 kWh.m^{-2}day^{-1} [5]. Thus, studying, modeling, simulating, dimensioning, designing adsorption solar refrigeration systems appear as promising solutions to answer the important issues of cold, the improvement of living conditions and the reduction of the excessive consumption of electrical energy [6]. Indeed, solar adsorption refrigeration units operate without moving parts and do not require any other energy source besides solar energy. The technology of these machines is simple, maintenance is easy and the manufacturing materials used are recyclable [7]. However, some disadvantages such

ISSN: 2277-9655
Impact Factor: 5.164
CODEN: IJESS7

as the discontinuous operation of the cycle [8-9], the poor heat and mass transfer in the adsorbent bed [10], the low thermal conductivity of the adsorbent [11] and the poor contact between the walls of the adsorber and the adsorbent [12-13] are obstacles to the transfer of technology and commercialization of these machines. Although many experimental and theoretical works have been carried out on solar adsorption refrigerators, the technology is not sufficiently mastered to the extent that the product has not been popularized. Moreover, the different models developed have been, most of the time, made in a fragmentary way, that is to say, either only the adsorber, or the condenser or the evaporator. To overcome this lack of control, the development of a global model of the different components of the adsorption solar refrigerator, as well as its dimensioning, is necessary in order to make suggestions that can propel the advancement of scientific research in this field. Thus, the main objective of this study is to model and simulate the operation of an adsorption solar refrigerator in order to evaluate and analyze its energy performance.

2. MATERIALS AND METHODS

2.1. Presentation of the model

Figure 1 presents the model of the adsorption solar refrigerator. It is composed of a collector-adsorber containing the adsorbent-adsorbate couple (zeolite-water), a condenser and an evaporator located in a refrigeration chamber.

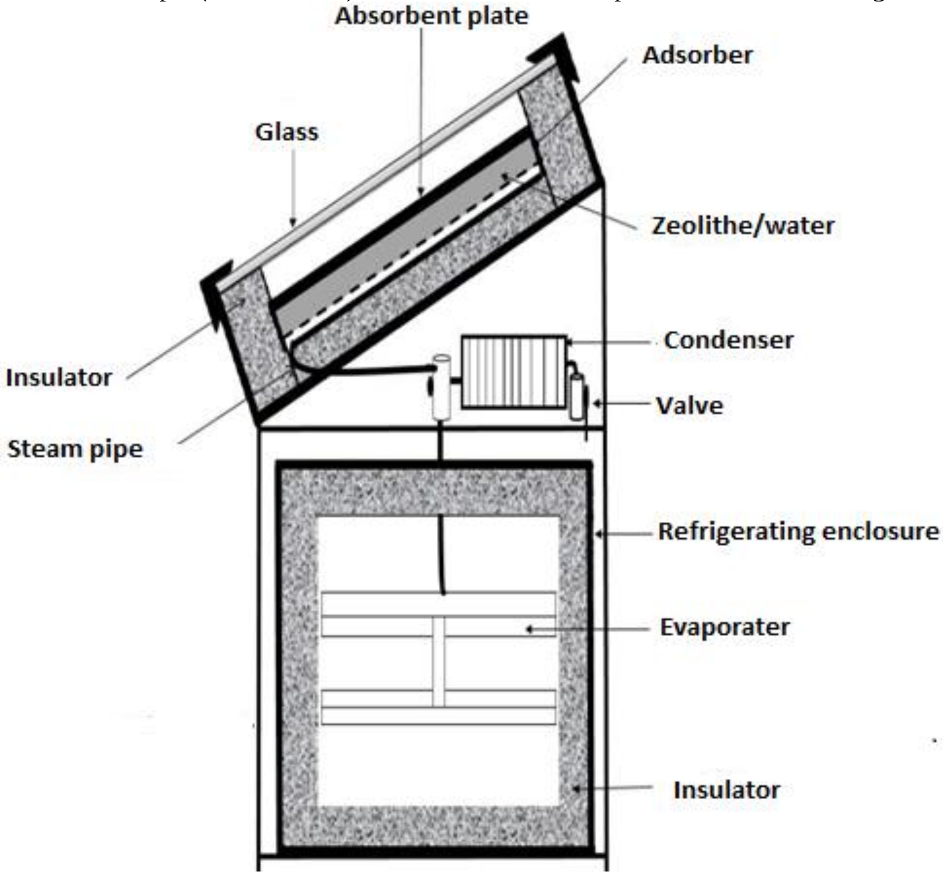

Fig 1: Schematic of the adsorption solar refrigerator

2.2. Working principle of the adsorption solar refrigerator

The adsorption solar refrigerator has a cyclic operation. Its operating principle is based on the phenomena of adsorption-desorption. This reaction is exothermic or endothermic depending on the direction of the process. This cycle (figure 2) describes the evolution of the state of the mixing level of the adsorbent/adsorbate couple contained in the refrigerator. It is composed of four main phases: the isosteric sensible heating, the sensible heating desorption, the isosteric sensible cooling and the sensible cooling adsorption.

ISSN: 2277-9655
Impact Factor: 5.164
CODEN: IJESS7

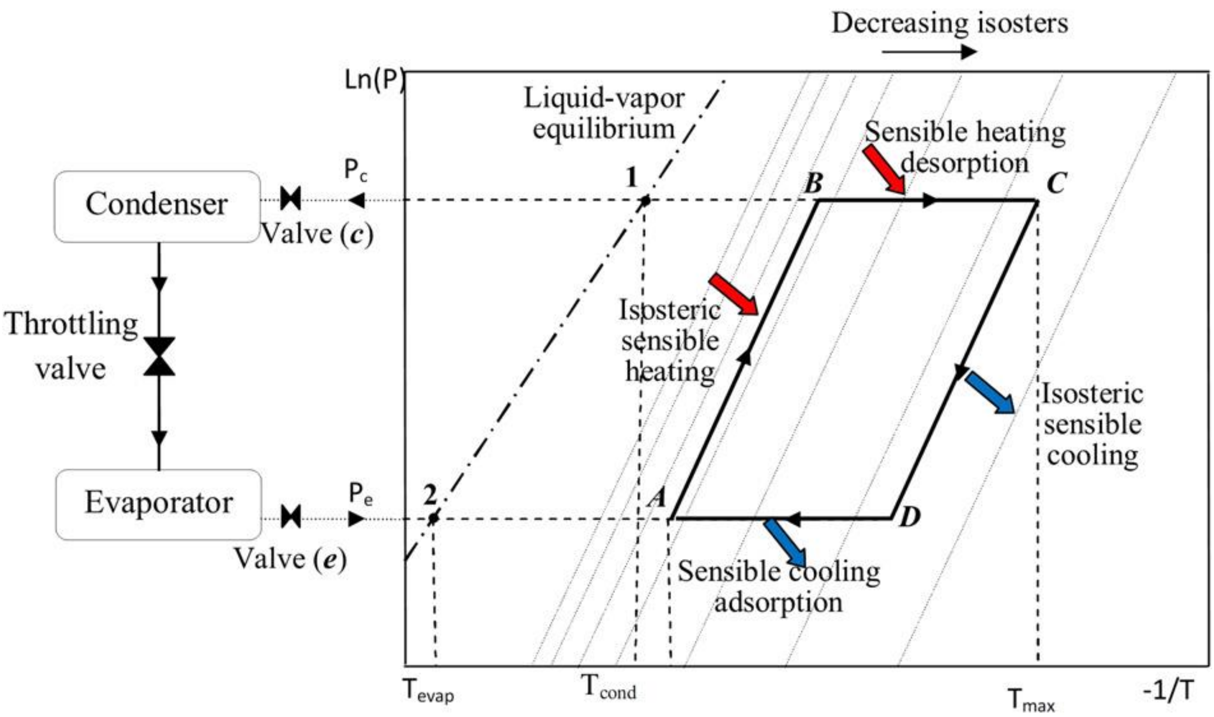

Fig 2: Clapeyron diagram for a conventional adsorption cycle [14]

3. MATHEMATICAL FORMULATION

The developed model is a so-called 'global' model. It takes into account the interaction between the elements which compose the refrigerating installation and allows to highlight the types of couplings existing between the latter. This model is based on the hypothesis that each element is characterized by quantities supposed to be uniform (nodal method). In our case, these quantities will be the temperature, the pressure and the mass of adsorbed water vapor.

3.1 Simplifying assumptions

To obtain an approximate simulation of the solar adsorption refrigerator, some assumptions have been proposed. These are :

- the porous material (adsorbent) is assimilated to a medium with a temperature T and an equivalent thermal conductivity;
- the heat transfer is unidirectional;
- the convective heat transfer and the pressure losses are negligible in the porous medium;
- the pressure remains constant in the condenser and in the evaporator;
- the total mass of desorbed adsorbate vapor condenses completely;
- the mass transfer resistance is negligible;
- the physical properties of the adsorbent and the metal walls of the adsorber, condenser and evaporator are considered constant.

3.2 Balance equations

→ ***Energy balance of glass***

$$m_v Cp_v \frac{\partial T_v}{\partial t} = \alpha_v . G_n . s_v + h_{p-v} . s_v \left(T_p - T_v\right) - h_{cv-v-ext} . s_v \left(T_v - T_{amb}\right) - h_{r-v-ciel} . s_v \left(T_v - T_{ciel}\right) \quad (1)$$

T_v is the temperature of the glass, T_p the temperature of the absorber plate and T_{amb} the temperature of the ambient environment.

→ ***Energy balance of absorber plate***

$$m_p Cp_p \frac{\partial T_p}{\partial t} = (\alpha\tau)_{eff}\, s_p G_n - h_{p-v} s_v (T_p - T_v) - h_{p-a} s_p (T_p - T) \quad (2)$$

Where T is the equilibrium temperature of the zeolite/water mixture and h_{p-a} the heat transfer coefficient between the absorber plate and this mixture.

→ ***Energy balance of adsorbent bed***

- During the isosteric heating and desorption phase

$$m_{eq} Cp_{eq} \frac{\partial T}{\partial t} = h_{p-a}.s_p (T_p - T) + \delta\left(\Delta H_{des}.m_a.\frac{\partial m^{des}}{\partial t} + m_a.Cp_l (T - T_{cd}).\frac{\partial m^{des}}{\partial t} \right) \quad (3)$$

- During the isosteric cooling phase and adsorption

$$m_{eq} Cp_{eq} \frac{\partial T}{\partial t} = h_{p-a}.s_p (T_p - T) + \delta\left(\Delta H_{ads}.m_a.\frac{\partial m^{ads}}{\partial t} - m_a.Cp_l (T - T_{ev}) \frac{\partial m^{ads}}{\partial t} \right) \quad (4)$$

With:

$\delta = 0$: During isosteric heating and cooling.
$\delta = 1$: During desorption and adsorption.

→ ***Condenser energy balance***

$$\left[m_{cd}.Cp_{cd} + m_d(t).Cp_l \right] \frac{\partial T_{cd}}{\partial t} = m_a.\frac{\partial m^{des}}{\partial t}\left[L_{cond}(P_{cd}) + Cp_l (T - T_{cd}) \right] - h_{r-cd-ciel}.S_{cd}(T_{cd} - T_{ciel}) - h_{cv-cd-amb}.S_{cd}(T_{cd} - T_{amb}) \quad (5)$$

Where $m_d(t)$ represents the total mass of adsorbate vapor desorbed, T_{cd} the temperature of the condenser and L_{cond} the latente heat of condensation.

→ ***Evaporator energy balance***

$$\left[m_{ev} Cp_{ev} + \left(m_d(t) - \Delta m.m_a \right) Cp_l \right] \frac{\partial T_{ev}}{\partial t} = -m_a \frac{\partial m^{ads}}{\partial t}\left[L_v (P_{ev}) - Cp_l (T - T_{ev}) \right] - h_{cv-ev-air} S_{ev} (T_{ev} - T_{air}) \quad (6)$$

Where T_{ev} is the temperature of the evaporator and L_v the latent heat of vaporization.

3.3 Kinetics model

The modeling of the adsorption cycle requires a good modeling of the phenomenon. It is thus essential to control the equilibrium parameters between the adsorbent and the adsorbate. This requires an appropriate choice of adsorption model allowing to describe correctly the adsorption properties of the couple used. A thorough examination led us to choose the phenomenological model of Dubinin- Astahkov which is the most suitable for the problem at hand. Thus the equation of the Dubinin- Astahkov model expressing the mass of adsorbate adsorbed on the surface of the adsorbent as a function of temperature (T) and pressure (P) is written:

ISSN: 2277-9655
Impact Factor: 5.164
CODEN: IJESS7

$$m = w_0 \rho_l(T) \exp\left(-D\left(T \ln \frac{P_s(T)}{P}\right)^n\right) \quad (7)$$

Where $\rho_l(T)$ is the density of the adsorbate (water), $P_s(T)$ the saturation pressure, W_0 the maximum adsorption capacity; D and n are constants depending on the adsorbent/adsorbate couple used. Using Antoine's equation giving the saturation pressure:

$$P_s(T) = 1000.\exp\left(16{,}89 - \frac{3803{,}9}{(T - 41{,}68)}\right) \quad (8)$$

3.4. System Coefficient of Performance

The solar coefficient of performance (COPs) of a solar refrigeration machine is defined as the ratio of the amount of cooling produced at the evaporator to the total incident solar energy during a full day.

$$COP_s = \frac{Q_f}{\int_{t_{sr}}^{t_{ss}} A_s.G_n.dt} \quad (9)$$

Where As is the collection area and Gn is the solar flux in W/m^2

Q_f the amount of cold produced at the evaporator, given by:

$$Q_f = m_a \Delta m\left[L(T_{ev}) - \int_{T_{ev}}^{T_{cd}} Cp_l(T)\,dT\right] \quad (10)$$

3.5. Initial Conditions

At the initial time, we assume that the temperatures of the components of the adsorber, the condenser and the evaporator are equal to the ambient temperature. The pressure in the adsorber is also assumed to be equal to the evaporation pressure corresponding to the saturation pressure at the evaporation temperature. Thus, for any, being the instant from which the collector-adsorber is subjected to the solar flux, we have:

$$T_v(t_0) = T_p(t_0) = T_{ev}(t_0) = T_{cd}(t_0) = T(t_0) = T_{amb} \quad (11)$$

$$P(t_0) = P_{ev} = P_s(T_{ev}) \quad (12)$$

$$m = m(T, P) \quad (13)$$

3.6. Numerical resolution

The method of solving the system of equations that describes the transient behavior of the model is purely numerical, based on the implicit finite difference method and the iterative method of Gauss Seidel. A computer program written in Fortran language has been developed to model and simulate on the one hand the adsorption-desorption kinetics of the zeolite/water couple and, on the other hand, the operation of each element of the refrigerator during one day.

4. RESULTS AND DISCUSSION

4.1 Analysis of the behavior of the different components of the adsorption solar refrigerator

The temporal evolution of the temperatures of the glass, the absorber plate, the adsorbent bed (zeolite), the condenser and the evaporator are represented in figure 3. At the beginning of the day, the temperatures are identical and equal to the adsorption temperature which, at sunrise, is equal to the ambient temperature. Under the action

ISSN: 2277-9655
Impact Factor: 5.164
CODEN: IJESS7

of the solar flux, the collector-adsorber heats up and the temperatures of its various components increase rapidly over time to reach a maximum value (Tv=358 K (85°C), Tp=396 K (123°C), Tzeo=395 K (122°C), Tcd=320 K). At the end of the day, the solar flux decreases and it results in a cooling of the collector-adsorber which starts as soon as the temperature of the adsorbent bed has reached the regeneration temperature. It can be seen that the temperatures of the different compartments of the adsorber decrease up to 300 K (27°C). This value represents the temperature at which there is no heat exchange between the glass, the plate and the adsorbent bed. The temperature of the evaporator decreases from about 297 K (24°C) to about 276 K (3°C). This drop in temperature is due to the evaporation of the condensate (water) which turns into steam and then flows towards the adsorbent bed. These same trends were found by Umair et al, (2014) who developed a solar refrigerator model using the activated carbon-ethanol couple [15].

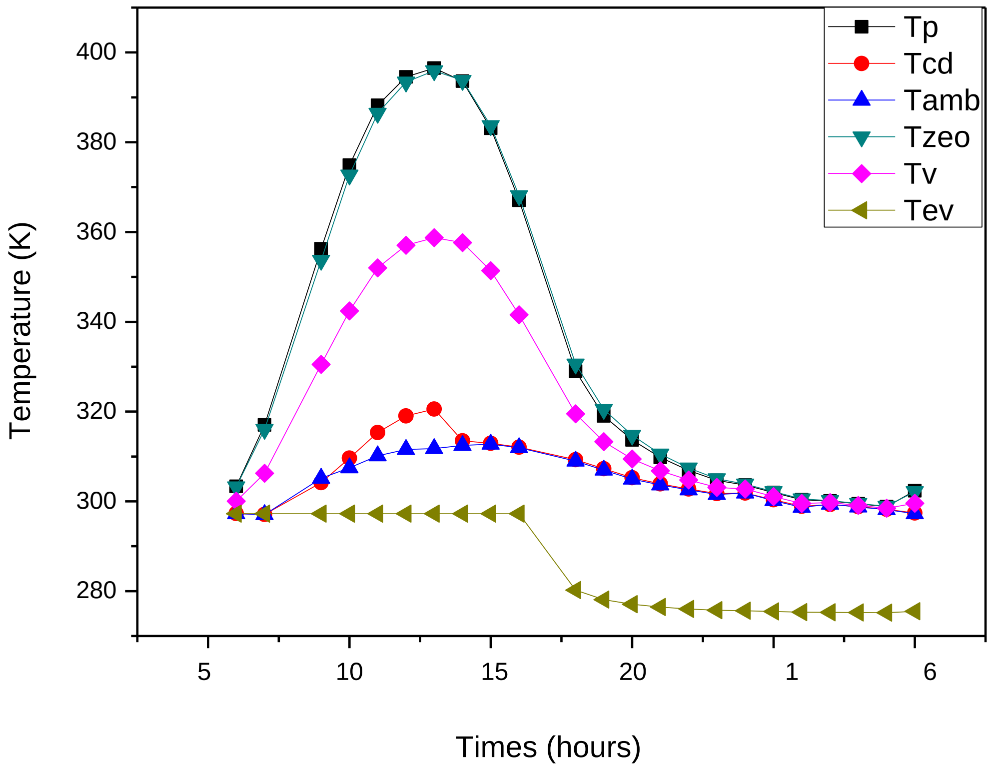

Fig 3: Temporal evolution of the temperature of the different components of the solar refrigerator.

4.2. Annual performance analysis of the solar adsorption refrigerator
To analyze the performance of our solar refrigerator over all periods of the year, we simulated the performance parameters over twelve (12) months of the year. These simulations were performed using the meteorological data of the year 1992-2006 and based on the notion of a typical day of the month [16].

4.2.1 Evolution of the operating parameters of the solar refrigerator during the different months of the year.
The temporal evolutions of the temperature of the adsorbent, the mass of adsorbed water vapor and the pressure of water vapor in the adsorber, during the twelve (12) months of the year, are respectively presented in Figures 4-6.

ISSN: 2277-9655
Impact Factor: 5.164
CODEN: IJESS7

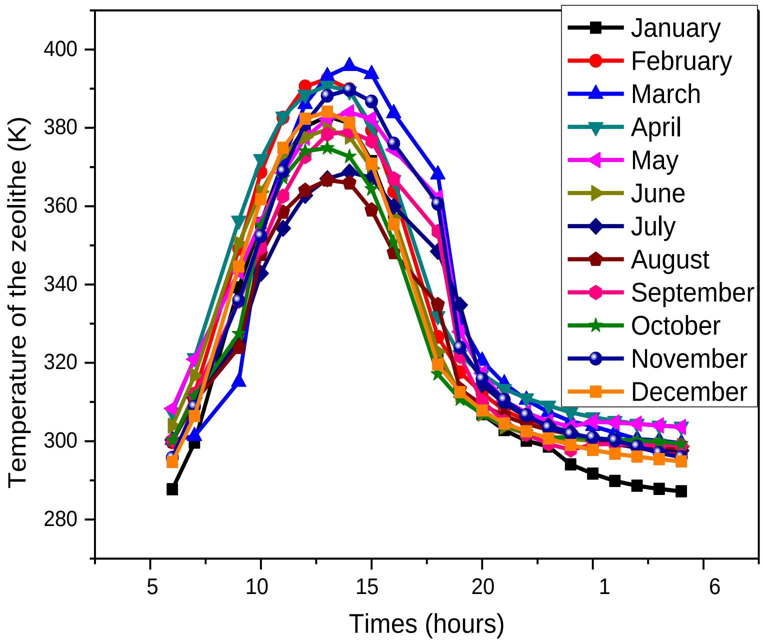

Fig.4. Temporal evolution of the zeolite temperature

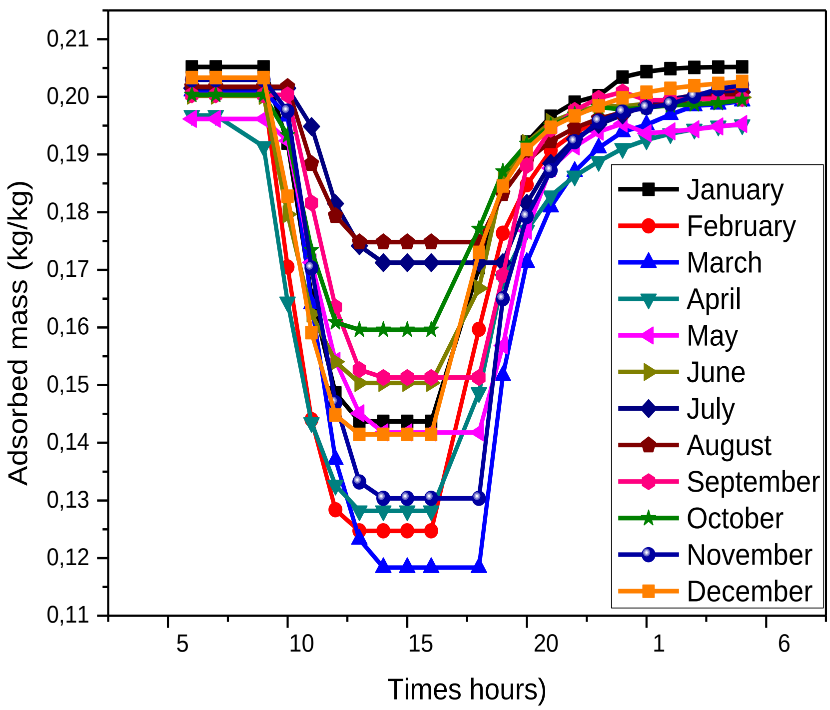

Fig.5. Temporal evolution of the adsorbed water vapor mass

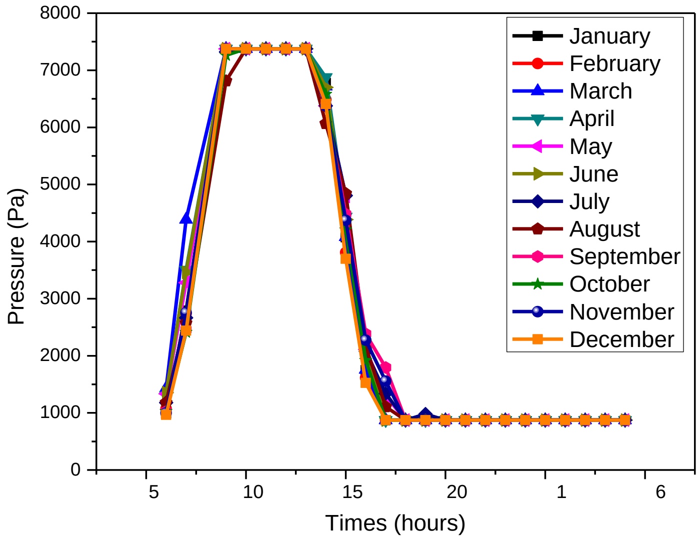

Fig.6. Temporal evolution of the water vapor pressure.

The profiles of the temperatures of the zeolite during the various months of the year have all the same aspect (figure 4). Under the action of the solar flux, the temperature of the zeolite increases progressively at the beginning of the day, then it reaches around 12 h, a respective maximum value of 395 K (122°C) for the month of March and 370 K (97°C) for the month of August, before decreasing until the end of the day.

The temporal evolution of the mass of water vapor adsorbed during the different months of the year are presented in Figure 5. It can be seen that these curves all have a similar appearance. Indeed, at the beginning of the cycle, the mass of water vapor adsorbed is almost constant and respectively equal to 0.201 kg/kg for the month of March and 0.198 kg/kg for the month of August. Then, it decreases progressively and reaches respectively, for the month of March and August, a minimum value of 0.115 kg/kg and 0.175 kg/kg, before starting to increase during the remaining phase of the cycle.

The evolutionary curves of the water vapor pressure during the different months of the year are presented in Figure 6. It is noted that the pressure increases while passing from the evaporation pressure Pev=872 Pa to the condensation pressure Pcd= 7376 Pa where it remains constant, then it decreases gradually until the end of the cycle.

The examination of these various curves shows that, for the month of March, the values of the temperature of the zeolite and the mass of water vapor cycled are higher than those obtained for the other months of the year. This finding can be justified by the fact that the solar irradiance values (990W/m^2) for this month are higher than those of the other months. Therefore, the amount of heat received by the adsorber allows the zeolite to reach higher temperature values (395 K), resulting in a significant desorption of water vapor. In addition, the pressure of the water vapor in the adsorber for this month increases rapidly to the pressure in the condenser. This results in an earlier start of the desorption-condensation phase.

Finally, we note that the climatic data have a great influence on the operation and thus, on the performances of the adsorption solar refrigerator. Indeed, when the climatic conditions are favourable (maximum solar flux), the mass of adsorbed water vapour ($m_{\min}$) at the end of the desorption phase decreases in the course of time because of the increase of the regeneration temperature. As a result, the mass of water vapor cycled Δm increases with solar irradiance. As a result, the amount of cold produced at the evaporator and the solar coefficient of performance increase with solar irradiance.

ISSN: 2277-9655
Impact Factor: 5.164
CODEN: IJESS7

4.2.2. Energy performance

In order to quantify the energy performance of the solar adsorption refrigerator, for optimal sizing, we evaluated the amount of cold produced at the evaporator and the solar coefficient of performance of the system for the twelve (12) months of the year. The COPs is the ratio between the amount of cold produced and the amount of heat supplied to the refrigeration machine. The COPs, Qf and Qc, calculated for the different months of the year, by the dynamic simulation using the meteorological data of typical days [16], are presented in Figure 7-8. It can be seen that the solar performance coefficients (COPs) obtained for all the months of the year (Figure 7) vary between 0.11 and 0.25. The maximum and minimum values are observed in March and August respectively. Indeed, during August, the solar radiation received by the sensor-adsorber is low due to cloud cover due to the rainy season. As a part of the energy received by the adsorber-catcher ensures the heating of the metal masses of the collector, the remainder is then insufficient for a good desorption of the water vapor. This results in a low cold production at the evaporator (2.11MJ) and thus a low COPs (0.11). On the other hand, for the month of March, the desorption of water vapour is important thanks to the high values of sunshine. Consequently, the amount of cold produced (6.39 MJ) and the COPs (0.25) are higher.

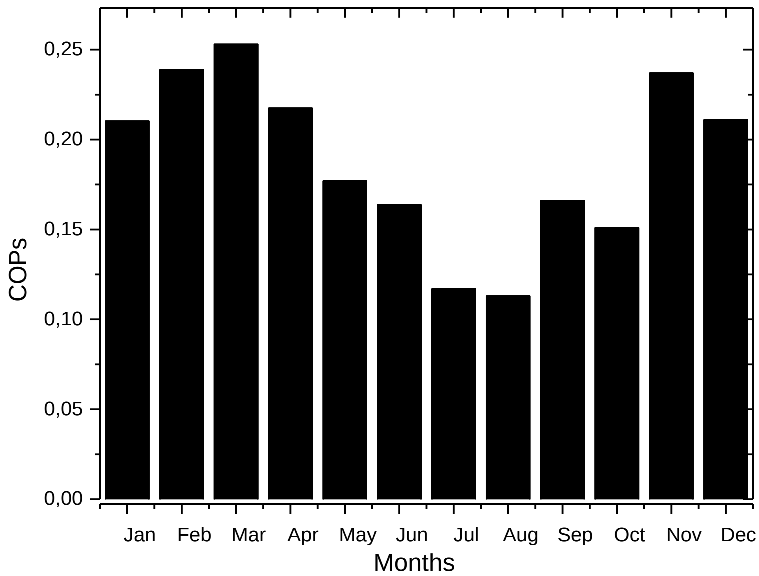

Fig.7. Simulated COPs over the 12 months of the year

Moreover, figure 8 shows the monthly evolution of the quantities of cold produced and the solar radiation received during the year. It is easy to see that the amount of cold produced and consequently the COPs are higher as the amount of solar energy captured by the collector-adsorber is higher. These results are in the order of magnitude given by the literature, through the work of authors (Table 1) such as Li et al, (2002) who carried out a theoretical study of a solar refrigerator, using the zeolite/water couple [17]. It appears from their study that the COPs varied from 0.25 to 0.30. Similarly, Hildbrand et al (2004) carried out an experimental study on a solar refrigerator using the silica gel-water couple with a silica gel mass of 78.8 kg. The refrigerator operates under the climatic conditions of Yverdon-les-Bains (Switzerland). The results obtained by these authors showed that the evaporator reached a minimum temperature of 0°C and the COPs varied between 0.12 and 0.23 [18].

ISSN: 2277-9655
Impact Factor: 5.164
CODEN: IJESS7

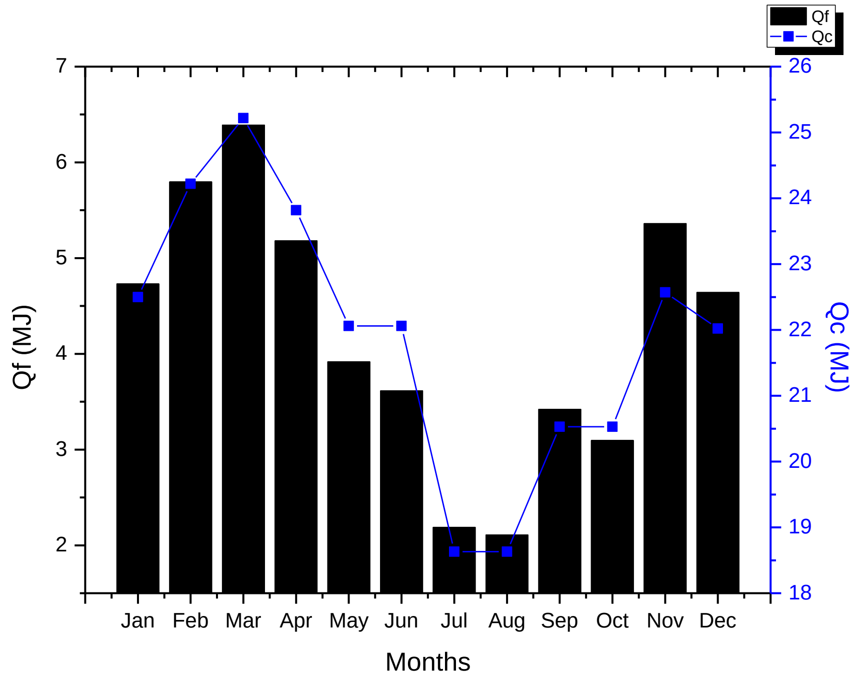

Fig.8. Quantity of cold produced Qf and quantity of heat received Qc during the 12 months of the year

Table 1: COPs of adsorption solar refrigerator

	Adsorbent/ adsorbate pair	**Insulator type**	**COPs**	**Solar energy (MJ/m^2)**
Present study	Zeolite/ water	Flat plate	0,11-0,258	16,6- 24 MJ/m^2
Li et al., 2002	Zeolite/ water	Pipes	0,25-0,30	---
Tchernev, 1982	Zeolite/ water	Flat plate	0,15	21,6 MJ/m^2
Grenier et al., 1988	Zeolite/ water	Flat plate	0,10	17,8-22 MJ/m^2
Hildbrand et al., 2004	Silica-gel/ water	Flat plate	0,12-0,23	> 20 MJ/m^2
Bouzeffour et al., 2016	Silica-gel/ water	Pipes	0,083-0,09	19 MJ/m^2
Li et al., 2004	Activated carbon/ methanol	Flat plate	0,13-0,15	17-20 MJ/m^2
Lemmini et Errougani 2005	Activated carbon/ methanol	Flat plate	0,04-0,08	15,3-25,5 MJ/m^2
Qasem, et El-Shaarawi., 2013	Activated carbon/ methanol	Pipes	0,12-0,24	19,5-28 MJ/m^2
Chekirou et al., 2007	Activated carbon/ methanol	Pipes	0,13-0,18	26,12 MJ/m^2

5. CONCLUSION

In this paper, we have studied the operation of an adsorption solar refrigerator through an energy analysis. The results show that the performance of the adsorption solar refrigerator depends on several parameters. Thus, with a maximum solar radiation of 990W/m^2, the maximum temperatures of the absorber plate, zeolite and condenser are 396 K (123°C), 395 K (122°C) and 320 K (47°C) respectively. The evaporator temperature can drop to a minimum temperature of 276 K (3°C). Furthermore, the simulation showed that the climatic conditions also have a great influence on the operation of the solar refrigerator. Thus, the amounts of cold produced, the average solar flux densities and the COPs during March and December are 6.391 MJ and 4.642 MJ, 590 W/m^2 and 514 W/m^2 and 0.25 and 0.21, respectively, relative to the values of the climate parameters. In the same way, with an average

ISSN: 2277-9655
Impact Factor: 5.164
CODEN: IJESS7

daily solar flux density of 436 W/m^2 and 480 W/m^2 respectively for the months of August and October, the COPs are respectively 0.11 and 0.15, with a total quantity of cold produced respectively of 2.12 and 3.1 MJ. These results thus obtained, will make it possible to dimension in an optimal way the solar refrigerator with adsorption.

REFERENCES

[1] Anyanwu, E. (2000). Environmental pollution: restructuring the refrigeration industry as a way out. Environment Protection Engineering, 26(4); 17-28. doi:10.1016/S0196-8904(02)0 0038-9
[2] Hassan, H. (2013). Energy analysis and performance evaluation of the adsorption refrigeration system. ISRN Mech. Eng, 2013, 704340. doi:10.1016/j.energy.2010.10.01
[3] Louajari, M., Mimet, A., Ouammi, A. (2011). Study of the effect of finned tube adsorber on the performance of solar driven adsorption cooling machine using activated carbon-ammonia pair. Appl. Energy, 88, 690–698. doi:10.1016/j.apenergy.2010.08.032.
[4] Zhang, L. (2000). A three-dimensional non-equilibrium model for an intermittent adsorption cooling system. Solar Energy, 69(1), 27-35.
[5] M. Ousmane, B. Dianda, S. Kam, A. Konfe, T. Ky et D. Bathiebo, « Experimental study in natural convection.,» Global Journal of Pure and Applied Sciences. , p. 21(2):155., 2015.
[6] Errougani Abdelmoussehel, Fabrication et expérimentation d'un réfrigérateur solaire à adsorption utilisant le couple charbon actif-méthanol dans le site de rabat. Thèse de doctorat en physique énergétique, Université Mohammed V, Rabat 2007.
[7] Chikouche, A. (2012). Using solar energy for refrigeration purposes in Algeria. 4th JIIRCRAC Proceeding. Refrigeration Science and Technology Proceedings.
[8] Meunier, F. (2001). Adsorptive cooling: a clean technology. Clean Prod. Proc. (3, 8-20).
[9] Anyanwu, E. (2003). Review of solid adsorption solar refrigerator I: an overview of the refrigeration cycle. Energ. Conv. Mgn., 44, 301-312. doi:10.1016/S0196-8904(02)000 38-9
[10] Fadar, A. E. (2015) Thermal behavior and performance assessment of a solar adsorption cooling system with finned adsorber. Energy, 83, 674-684.
[11] Jemni, A., Ben Nasrallah, S. (1995). Study of two-dimensional heat and mass transfer during desorption in a metal- hydrogen reactor. Int. J. Hydrogen Energy, Vol. 20, pp 881- 891.
[12] Critoph, R., Turner, L. (1995). Heat transfer in granular activated carbon beds in the presence of adsorbable gases. Int. J. Heat Tran, 38 (9), 1577-1585. doi: 10.1016/0017-93 10(94) 00 276-2
[13] Almers, A., Azzabakh, A., Mimet, A. (2006). Optimal design study of cylindrical finned reactor for solar adsorption cooling machine working with activated carbon-ammonia pair. Applied thermal engineering, 26, 1866 - 1875. doi: 10.1016@j.applthermaleng. 2006. 01.021
[14] H.Z. Hassan, A.A. Mohamad, R. Bennacer (2011). Simulation of an adsorption solar cooling system. Energy 36, 530-537; doi:10.1016/j.energy.2010.10.011
[15] Umair, M., Akisawa, A., Ueda, Y. (2014). Performance evaluation of a solar adsorption refrigeration system with a wing type compound parabolic concentrator. Energies, 7,1448–1466. https://doi.org/10.3390/en7031448
[16] Ouedraogo, E., Coulibaly, O., Ouedraogo, A. (2012). Elaboration d'une année météorologique type de la ville de Ouagadougou pour l'étude des performances énergétiques des bâtiments. Revue des Energies Renouvelables, 15, 77-90.
[17] Li, M., Wang, R., Xu, Y., Wu, J., Dieng, A. (2002). Experimental study on dynamic performance analysis of a flat-plate solar solid-adsorption refrigeration for ice maker. Renewable Energy, 27, 211–221. doi:10.1016/ S0960-1481(01)00188-4.
[18] Hildbrand, C., Dind, P., Pons, M., Buchter, F. (2004). A new solar powerd adsorption refrigerator with high performance. Solar Energy, , vol 77, pp.311-318.
[19] Tchernev, D. (1982). Solar air conditioning and refrigeration systems utilizing zeolites. Proc. Meetings of IIR Commissions E1-E2 , pp. 209–215.
[20] Grenier, P., Guilleminot, J.J, Meunier, F., Pons, M. (1988). Solar powered solid adsorption cold store. Journal of Solar Energy Engineering, Vol 110, pp.192-197.
[21] Bouzeffour, Fatih; Khelidj, Benyoucef; Tahar, Miloud (2016). Experimental investigation of a solar adsorption refrigeration system working with silicagel / water pair: A case study for Bou-Ismail solar data. Solar Energy 131, 165-175. doi : 10.1016/j.solener.2016. 02.043 .

ISSN: 2277-9655
Impact Factor: 5.164
CODEN: IJESS7

[22] Li, M., Sun, C., Wang, R., Cai, W. (2004). Development of no valve solar ice maker. Appl Therm Eng, 24(5-6), 865–72. doi:10.1016/j.applthermaleng.2003.10.002.
[23] Qasem, N., El-Shaarawi, M. (2013). Improving ice productivity and performance for an activated carbon/methanol solar adsorption ice-maker. Sol. Energy, 98, 523–542. doi:10.1016/j.solener.2013.10.018.